Daily Avalanche Probability Indication Maps: First Operational Experience in Davos, Switzerland

Julia Glaus*[1], Pia Ruttner[1,2,4] , Lukas Stoffel[1], Johan Gaume[1,2,3], Yves Bühler[1,2]

[1] *WSL Institute for Snow and Avalanche Research SLF, Grisons, Switzerland*
[2] *Climate Change, Extremes, and Natural Hazards in Alpine Regions Research Centre CERC, Grisons, Switzerland*
[3] *Institute for Geotechnical Engineering ETH Zurich, Zurich, Switzerland*
[4] *Institute of Geodesy and Photogrammetry ETH Zurich, Zurich, Switzerland*

ABSTRACT:

Avalanche risk management in ski resorts, along traffic routes, and for exposed buildings relies mainly on point-based measurements, field observations, avalanche cadastres, avalanche bulletins, and expert judgment, particularly during storms with limited visibility. At Brämabüel (Davos), three major avalanche paths threaten a cross-country ski track and the Dischma road, requiring timely operational decisions such as road closures or avalanche control, which could have considerable economic impact. During the 2025/26 winter season, we implemented and tested an operational workflow that generates daily, spatially explicit probability indication maps of avalanche runout for direct use by local experts. The approach relies on an avalanche dynamics model that simulates both snow entrainment and the powder cloud. The model is driven by snowpack simulations forced by meteorological station data, low-cost lidar sensor and camera imagery. By coupling dynamic avalanche modeling with measurement-based information on snow cover, the framework provides a practical tool for near-real-time hazard assessment. During a storm event from 16–22 February, a spontaneous avalanche released at night, significantly depleting the release area. A subsequent artificial release remained small. Such changes in snow depth, which strongly affect avalanche formation and release, are not captured by station-based modeling. The lidar information helps to interpret the probability indication maps of the following days or even provides the basis to update them. This case study demonstrates how integrating modeling and remote sensing improves situational awareness and supports more robust decision-making under challenging observational conditions such as snowfall. The approach adds a complementary perspective for practitioners and will be tested across larger regions and different climatic conditions, while its effective use depends on defining robust decision thresholds (e.g., for road closures) in close collaboration with practitioners.

KEYWORDS: Avalanche Dynamics, Road Safety, Forecasting, Probability, Hazard Assessment

1. INTRODUCTION

Operational avalanche control during prolonged snowfall events remains challenging, particularly when visibility is low or absent and direct assessment of snow conditions in release zones is not possible. In such situations, local experts must decide whether ski runs, transport routes, or exposed infrastructure can remain open, need to be closed, or require active avalanche control (Margreth, 2021). An important parameter is the amount of recent new snow stored in the release areas and avalanche tracks.

Probabilistic approaches have long been used to account for variability in avalanche occurrence and runout. For example, Keylock et al., 1999 used extreme-value statistics and frequency–magnitude relationships to estimate exceedance probabilities for avalanche runout distances. More recent approaches increasingly combine observations, snowpack information, and numerical avalanche simulations to estimate potential runout under current conditions (Vera Valero et al., 2016; Sheng et al., 2022; Mariani et al., 2024). Such approaches provide a basis for moving from long-term hazard assessment towards model-based support for operational avalanche decisions.

In this paper, we apply a probabilistic framework that combines meteorological station data, weather forecasts, snowpack simulations, and avalanche-dynamics simulations to provide daily forecasts of potential avalanche runout. The approach uses information from several meteorological stations in the Davos region to estimate the amount and properties of snow available for release. These estimates are used as input for avalanche-dynamics simulations, resulting in daily probability indication maps of potential avalanche runout.

Building on the frequency-based approach of (Glaus, Kleinn, et al., 2026), we implemented the methodology operationally during winter 2025/26 at Brämabüel, Davos. Probability indication maps were calculated once per day using the snow and

* *Corresponding author address:*
Julia Glaus
WSL Institute for Snow and Avalanche Research SLF
7260 Davos Dorf, Switzerland;
tel: +41 81 4170 378
email: julia.glaus@slf.ch

weather information available at the time of calculation. Each map represents the 24-h period from 12:00 on the respective day to 12:00 on the following day.

We focus on the snowfall period from 16–22 February 2026. During the night from 16 to 17 February, a large spontaneous avalanche released on the Brämabüel slope, followed by an artificial release five days later. These events provide a test case for comparing the simulation-based avalanche probability indication maps with the observed avalanche activity.

2. METHODS

2.1. Study area and observations

The Brämabüel slope is located above the Dischma valley near Davos, Switzerland. Several avalanche paths descend towards a cross-country track and the Dischma road. The cross-country track lies within the runout area above the road, while avalanches reaching the road subsequently flow into the counter-slope. We focus on the Wildi (track 1) and Rüchi (track 2) avalanche paths, shown in Figure 1. The location is described in more detail in (Glaus, Wikstrom Jones, et al., 2025). Forest is not represented in the avalanche simulations. Runout in track 3 is therefore overestimated, as the braking effect of the forest is neglected. We show the results for completeness but focus mainly on track 1 and 2 in the discussion.

2.2. Daily snow and weather conditions

Meteorological observations were obtained from measurement stations in the Davos region (Table 1). In addition, hourly terrestrial lidar measurements were available for the Brämabüel slope based on the setup presented in (Ruttner, Voordendag, et al., 2025). Differences between lidar measurements before and after an avalanche provide spatial information on changes in snow height in the release areas, avalanche tracks, and deposition areas.

For each prediction day, we used SNOWPACK (Bartelt et al., 2002) simulations from seven IMIS stations (Table 1). We evaluated the snowpack simulations using information available before the respective prediction period. Meteorological forecast data were then added for the following 24 h. We represented potential additional loading from wind-drifted snow with different wind-drift scenarios. For each station, we considered two potential weak layers: the interface between the new snow and the old snowpack and the most unstable weak layer in the old snowpack.

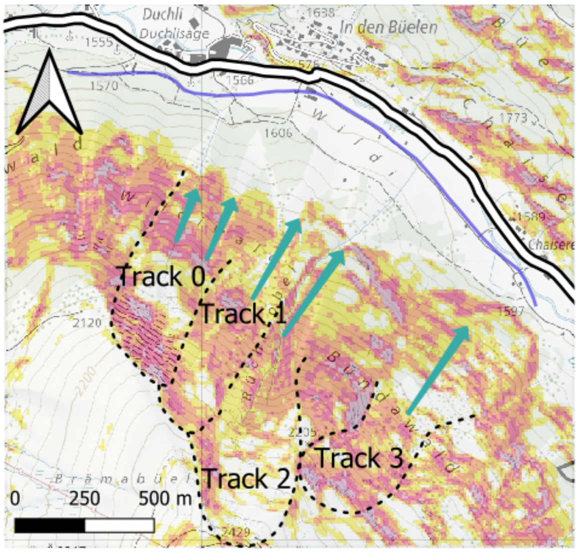

Figure 1: Overview of the Brämabüel slope with the four avalanche paths. Track 0 is protected by avalanche fences, track 1 is called Wildi, track 2 Rüchi and track 3 Chaiseren. The road is shown as a white line with black borders, while the cross-country ski-trail network is represented schematically by a single violet line.

Table 1: Overview of the IMIS stations used to derive the daily snowpack scenarios at Brämabüel including the distance to the Brämabüel slope.

Station	***Elevation m a.s.l.***	***Distance km***
SLF	1563	3.0
Weissfluhjoch	2536	5.6
Bärentälli	2558	9.9
Hanengretji	2455	5.6
Frauentobel	2330	4.8
Lukschalp	2290	3.4
Kreuzweg	2290	8.0

2.3. Frequency approach

The probability indication maps were calculated using the frequency approach described by Glaus, Kleinn, et al. (2026). The fracture depths obtained from the different stations, weak-layer types, forecast conditions, and wind-drift scenarios were grouped into 0.1 m bins. Their relative frequency defines the weight assigned to each fracture-depth class. The predicted snow temperatures were assigned to the corresponding temperature classes in the same way.

2.4. Avalanche simulations and probability indication maps

Avalanche runout was obtained from pre-calculated RAMMS::Extended simulations covering the considered fracture-depth and snow-temperature bins as defined above. The simulations include snow entrainment and the powder-snow component. The maximum entrainment depth was assumed to correspond to the deepest detected weak layer. Snow density in the release area was estimated from SNOWPACK and assumed to be constant along the entire avalanche path. The simulations were performed on a 5 m grid. The simulated powder clouds remained weak throughout the simulation scenarios and are therefore not shown.

For each day, simulations corresponding to the predicted fracture depth and snow-temperature distributions were selected and weighted by their respective frequencies. The weighted simulation results were combined to generate a spatial probability indication map for the following 24 h. The procedure was repeated each day from 16–22 February 2026.

Two potential release area (PRA) scenarios were considered, denoted Small and Medium PRA (Bühler et al., 2018). In addition to the spatial maps, the probability that the simulated avalanche core reaches the Dischma road was extracted along the road. This provides the probability indication directly at the area of interest.

2.5. Predicted snow conditions

The predicted fracture-depth distributions vary throughout the event, with most scenarios between approximately 0.5 and 1.5 m. Snow temperatures are mainly between -9 and $-5\,^{\circ}$C.

The distributions change as new snow accumulates, the existing weak layers are loaded, and the forecast temperature and wind conditions change. Avalanche activity within the Brämabüel slope does not automatically modify these input distributions.

3. RESULTS

3.1. Daily probability indication maps

A persistent weak layer had dominated the snowpack structure throughout the winter season up to the analysed event. Snowfall beginning on 14 February in the evening added load to this snowpack and continued during the following days. Figure 2 shows the evolution of total snow height, 12-h new snow height, and air temperature at Weissfluhjoch. At the beginning of the event, total snow height was approximately 105 cm. Snowfall intensified during 16 February and continued through 17 and 18 February, increasing the total snow height to approximately 180 cm. The largest 12-h new-snow amounts reached approximately 30–35 cm, while air temperature remained well below $0\,^{\circ}$C. After a temporary decrease in snow height on 18 and 19 February, further snowfall occurred on 19–20 February and again on 21–22 February. Total snow height reached approximately 190 cm during the latter period, while air temperature increased and approached $0\,^{\circ}$C on 22 February.

The resulting probability indication maps are shown in Figure 4. The two map columns show the Small and Medium PRA scenarios; the avalanche bulletin and observed avalanche activity are given in the right column. For both PRA scenarios, the largest probabilities occur within the established avalanche tracks, and the probability indication increases during the first part of the snowfall period.

The calculation for 16 February represents the period from 12:00 on 16 February to 12:00 on 17 February. During this prediction period, a spontaneous avalanche released on the Brämabüel slope. The avalanche largely depleted the Wildi release area, leaving little snow in place, and also removed part of the snow cover in the Rüchi release area. Direct observation was not possible because of the ongoing snowfall and poor visibility. Comparison of lidar measurements before and after the event indicates that large parts of the snow cover in the release areas were removed and constrains the occurrence of the avalanche to before approximately 02:00 on 17 February. The measurements are presented in detail in (Ruttner, Wieser, et al., 2024).

Snowfall continued after the avalanche, and the meteorological measurements therefore indicated further loading. The probability indication maps calculated after the event continued to use the snow conditions derived from the station data and not from the Lidar. The calculations shown in Figure 4 do not account for the reduced snow depth in the release zones.

3.2. Probability indication along the road

The spatial maps show whether individual avalanche paths approach or reach the road, but the differences between days are easier to quantify directly along the road. Figure 3 therefore shows the probability that the avalanche core reaches each position along the analysed road section.

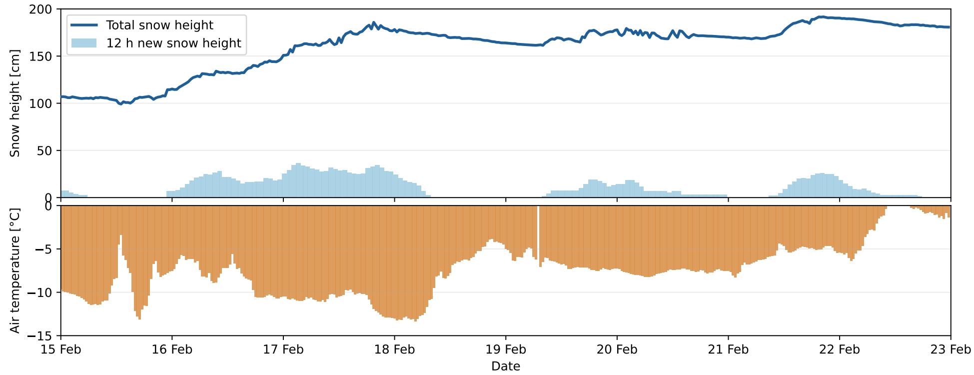

Figure 2: Measurements at IMIS station Weissfluhjoch of total snow height, 12-h new snow height, and air temperature from 15–23 February 2026.

The shaded areas denote four sections in which avalanche tracks intersect the road.

For the Small PRA, the largest values occur in track 3 at approximately 2.35 km along the road. The maximum probability indication reaches about 60–65% on 17 and 18 February. Tracks 0–2 show lower values, generally below approximately 35%. The probability indication decreases during the later part of the snowfall period till the 21st as there was an increase in temperature.

The Medium PRA produces higher values along the road and affects a larger fraction of the road section. The temporal development remains similar to the Small PRA, with the largest values during the first part of the snowfall period.

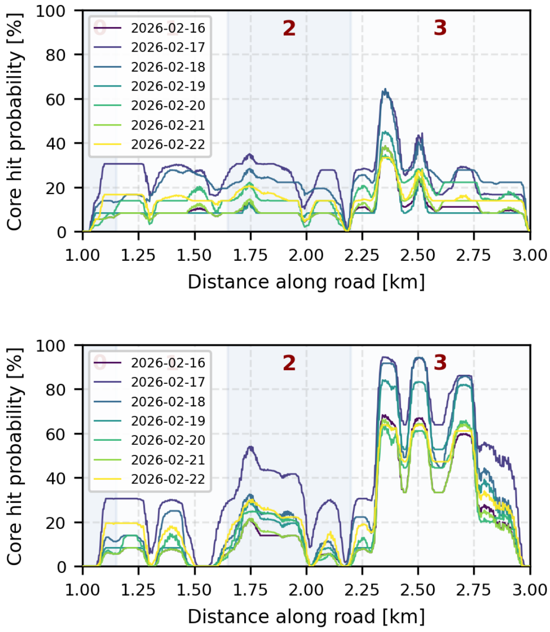

Figure 3: Probability that the avalanche core reaches the Dischma road for the small PRA (top) and the medium PRA (lower) scenarios from 16–22 February 2026. The shaded areas indicate the avalanche-track sections intersecting the analysed road section. The labels for track 0 and 1 are hidden behind the legend.

4. DISCUSSION

The daily probability indication maps provided spatially and temporally varying estimates of potential avalanche runout during the snowfall period from 16–22 February 2026 as shown in Figure 4 The highest calculated probabilities occurred during the period with the largest observed avalanche activity the 17 February 2026, and the maps identified the sections of the Dischma road most exposed to the individual avalanche paths.

The probability indication maps cannot yet be directly translated into a threshold for road closure. Their interpretation also depends on information that is currently not included in the calculation, such as recent avalanche activity and local changes in the snow cover. In future implementations, such information could be incorporated by updating the fracture depth in individual release areas from lidar observations. Where the remaining snow cannot be quantified reliably, recently active avalanche paths could instead be indicated directly on the probability indication maps.

The calculated probabilities further depend on how well the avalanche-dynamics simulations represent the individual avalanche paths. This is particularly evident for track 3 (Chaiseren), where the simulated probability of reaching the road is considerably higher than for the other paths. Forest and low vegetation within this path are not repre-

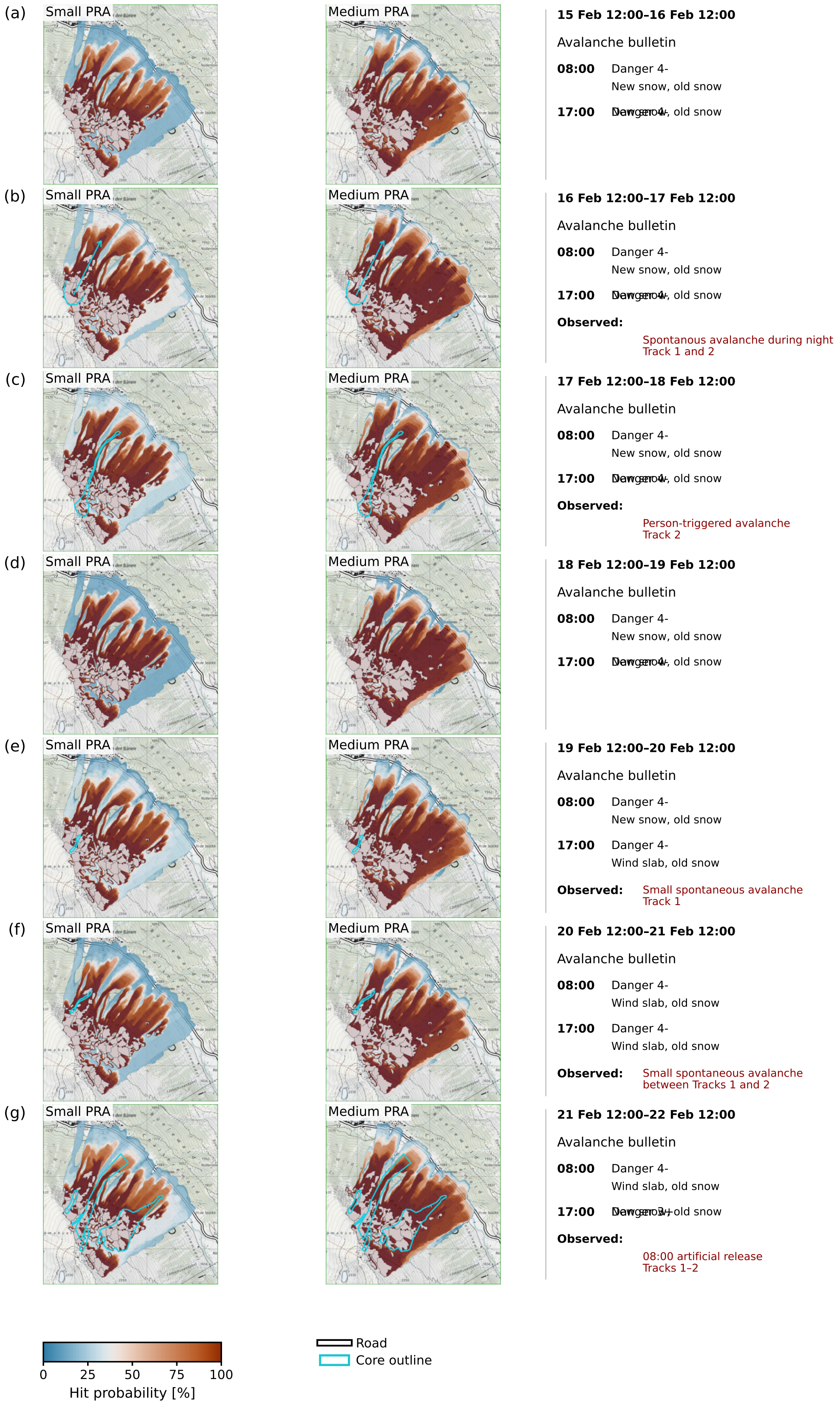

Figure 4: Daily probability indication maps with the avalanche bulletin and observed avalanche activity.

sented in the simulations, although they increase the friction to avalanche flow. Simulations using the standard friction parameters therefore tend to overestimate runout in this path. Such path-specific limitations need to be considered when interpreting the probability indication values.

The probability indication maps presented here were calculated from pre-calculated RAMMS::Extended simulations. The tool includes snow entrainment and the powder-snow component, but requires a comparatively detailed parameterization of the avalanche dynamics. The probability-mapping framework itself is not restricted to a specific simulation tool. In principle, other avalanche-dynamics models can be used to feed the inputs files. For applications focusing on cold-snow avalanches, simpler avalanche-dynamics models that include snow entrainment, such as MoT-PRA (Vicari et al., 2025) or com1DFA (Tonnel et al., 2023), could therefore also be considered.

5. CONCLUSIONS

The probability indication maps provide spatial information on potential avalanche runout under the predicted snow conditions. This is particularly useful during prolonged snowfall and poor visibility, when direct observation of the release areas and avalanche tracks is limited or impossible. The maps also identify the sections of the road that are most exposed to individual avalanche paths and therefore provide local experts with additional information for the operational assessment.

For operational application, the maps need to be interpreted together with observations of avalanche activity and local snow-cover conditions. The analysed event showed that lidar observations can provide information that is not contained in station-based snowpack simulations and could in future be incorporated directly into the probability indication maps. Further evaluation over snowfall periods with different levels of avalanche activity is required before probability levels can be related to operational measures such as road closure.

ACKNOWLEDGEMENTS

We first thank Vali Meier for keeping us informed about the avalanche control activities at Brämabüel and the artificially released avalanches. We thank Mathias Bavay for providing the SNOWPACK simulations and Marc Christen for valuable discussions and for setting up the latest version of RAMMS::EXTENDED for large-scale calculations. We also thank Tobias Jonas, Nander Wever, and Oliver Fuhrer (MeteoSwiss) for providing the forecast data, and Frank Techel for his support in identifying weak layers from SNOWPACK. We acknowledge the use of generative AI tools for assistance in improving the grammar and writing style of the manuscript. This research was funded by the Swiss National Science Foundation (SNSF) under project number 207519, "Avalanche Safety for Roads".

REFERENCES

Bartelt, P. and Lehning, M. (Nov. 2002). A Physical SNOWPACK Model for the Swiss Avalanche Warning: Part I: Numerical Model. In: Cold Regions Science and Technology 35.3, pp. 123–145. ISSN: 0165-232X. https://doi.org/10.1016/S0165-232X(02)00074-5.

Bühler, Y., von Rickenbach, D., Stoffel, A., Margreth, S., Stoffel, L., and Christen, M. (Dec. 2018). Automated Snow Avalanche Release Area Delineation – Validation of Existing Algorithms and Proposition of a New Object-Based Approach for Large-Scale Hazard Indication Mapping. In: Natural Hazards and Earth System Sciences 18.12, pp. 3235–3251. ISSN: 1561-8633. https://doi.org/10.5194/nhess-18-3235-2018.

Glaus, J., Kleinn, J., Stoffel, L., Ruttner, P., Wikstrom Jones, K., Gaume, J., and Bühler, Y. (Mar. 2026). Probabilistic Avalanche Runout Modelling for Daily Risk Management of Traffic Routes. In: EGUsphere, pp. 1–29. https://doi.org/10.5194/egusphere-2026-999.

Glaus, J., Wikstrom Jones, K., Bartelt, P., Christen, M., Stoffel, L., Gaume, J., and Bühler, Y. (July 2025). Simulation of Cold-Powder Snow Avalanches Considering Daily Snowpack and Weather Situations. In: Natural Hazards and Earth System Sciences 25.7, pp. 2399–2419. ISSN: 1561-8633. https://doi.org/10.5194/nhess-25-2399-2025.

Keylock, C. J., McClung, D. M., and Magnússon, M. M. (1999). Avalanche Risk Mapping by Simulation. In: Journal of Glaciology 45.150, pp. 303–314. ISSN: 0022-1430, 1727-5652. https://doi.org/10.3189/002214399793377103.

Margreth, S. (Jan. 2021). Lawinengefahrenkarten in Der Schweiz - Avalanche Hazard Maps in Switzerland. In: 184, pp. 80–92.

Mariani, A., Dellarole, L., Villa, G., Borsotti, J., and Monti, F. (Sept. 2024). A NEW OPERATIONAL APPROACH FOR THE DAILY ASSESSMENT OF POTENTIAL AVALANCHE DANGER. In: International Snow Science Workshop 2024, Tromsø, Norway, pp. 116–123.

Ruttner, P., Voordendag, A., Hartmann, T., Glaus, J., Wieser, A., and Bühler, Y. (Apr. 2025). Monitoring Snow Depth Variations in an Avalanche Release Area Using Low-Cost Lidar and Optical Sensors. In: Natural Hazards and Earth System Sciences 25.4, pp. 1315–1330. ISSN: 1561-8633. https://doi.org/10.5194/nhess-25-1315-2025.

Ruttner, P., Wieser, A., Glaus, J., and Bühler, Y. (2024). Near Real-Time Snow Depth Monitoring with Low-Cost Lidar Sensors for Road Safety Decisions. In: ISSW.

Sheng, J., Mind'je, R., Zhang, X., Wang, Y., Zhou, H., and Li, L. (Sept. 2022). Implementation of an Early Warning for Snowfall-Triggered Avalanche to Road Safety in the Tianshan Mountains. In: Cold Regions Science and Technology 204, p. 103675. https://doi.org/10.1016/j.coldregions.2022.103675.

Tonnel, M., Wirbel, A., Oesterle, F., and Fischer, J.-T. (Nov. 2023). AvaFrame *com1DFA* (v1.3): A Thickness-Integrated Computational Avalanche Module – Theory, Numerics, and Testing. In: Geoscientific Model Development 16.23, pp. 7013–7035. ISSN: 1991-959X. https://doi.org/10.5194/gmd-16-7013-2023.

Vera Valero, C., Wever, N., Bühler, Y., Stoffel, L., Margreth, S., and Bartelt, P. (Nov. 2016). Modelling Wet Snow Avalanche Runout to Assess Road Safety at a High-Altitude Mine in the Central Andes. In: Natural Hazards and Earth System Sciences 16.11, pp. 2303–2323. ISSN: 1561-8633. https://doi.org/10.5194/nhess-16-2303-2016.

Vicari, H. and Issler, D. (2025). MoT-PSA: A Two-Layer Depth-Averaged Model for Simulation of Powder Snow Avalanches on 3-D Terrain. In: Annals of Glaciology 65, e16. ISSN: 0260-3055, 1727-5644. https://doi.org/10.1017/aog.2024.10.